

Potential of electron transfer and its application in dictating routes of biochemical processes associated with metabolic reprogramming

Ronghui Yang^{1,3}, Guoguang Ying (✉)^{4,5,6}, Binghui Li (✉)^{1,2,3}

¹Department of Biochemistry and Molecular Biology, Capital Medical University, Beijing 100069, China; ²Advanced Innovation Center for Human Brain Protection, Capital Medical University, Beijing 100069, China; ³Beijing Key Laboratory for Tumor Invasion and Metastasis, Capital Medical University, Beijing 100069, China; ⁴Department of Cancer Cell Biology, Tianjin Medical University Cancer Institute and Hospital, Tianjin 300060, China; ⁵Key Laboratory of Breast Cancer Prevention and Therapy, Tianjin Medical University, Ministry of Education, Tianjin 300060, China; ⁶National Clinical Research Center for Cancer, Tianjin Medical University Cancer Institute and Hospital, Tianjin 300060, China

© Higher Education Press 2021

Abstract Metabolic reprogramming, such as abnormal utilization of glucose, addiction to glutamine, and increased *de-novo* lipid synthesis, extensively occurs in proliferating cancer cells, but the underneath rationale has remained to be elucidated. Based on the concept of the degree of reduction of a compound, we have recently proposed a calculation termed as potential of electron transfer (PET), which is used to characterize the degree of electron redistribution coupled with metabolic transformations. When this calculation is combined with the assumed model of electron balance in a cellular context, the enforced selective reprogramming could be predicted by examining the net changes of the PET values associated with the biochemical pathways in anaerobic metabolism. Some interesting properties of PET in cancer cells were also discussed, and the model was extended to uncover the chemical nature underlying aerobic glycolysis that essentially results from energy requirement and electron balance. Enabling electron transfer could drive metabolic reprogramming in cancer metabolism. Therefore, the concept and model established on electron transfer could guide the treatment strategies of tumors and future studies on cellular metabolism.

Keywords metabolic reprogramming; potential of electron transfer; cell proliferation; aerobic glycolysis; cancer metabolism

Introduction

Proliferating cells, such as cancer cells, require increased nutrients for intracellular biomass accumulation. Therefore, they need to upregulate the uptake of nutritional bricks and rewire the intracellular metabolic pathways relative to those of non-proliferating cells, known as “metabolic reprogramming” [1–3]. With the special context of rapid growth, poor vasculature and complex microenvironments, cancer cells tend to develop unusual metabolic behavior [4–7], such as abnormal glucose metabolism [8], ectopic utilization of alanine [9] and branched-chained amino acid [10,11], active proline

synthesis [4,12–14], and *de-novo* lipid synthesis from glutamine [15–18] or acetate [19–23]. Such metabolic changes are usually recognized as instructed by specific physiological, including molecular and biochemical signals.

Metabolic reprogramming, as a hallmark of cancers, occurs highly heterogeneously, and it is determined by diverse signal pathways [4,24–26]. Although blocking such pathways and the corresponding phenotypes could be possibly blocked in accordance with each individual context, such blockade usually appears as transient due to the development of eventual compensation effects between the pathways, particularly in *in-vivo* conditions. This phenomenon of metabolic compensation is an example when dealing with an autonomous self-adopting system, such as cancer, and equivalent types of frustration are usually encountered when other types of cancer pathways are focused for therapeutic targeting, including

Received December 1, 2020; accepted April 25, 2021

Correspondence: Guoguang Ying, yingguoguang@tmu.edu.cn;
Binghui Li, bli@ccmu.edu.cn

those involved in growth, metastasis, and drug resistance. In all these situations, multiple pathways exist, and each of them may take equivalent and sufficient roles in functioning and thus become substitutable but not indispensable. In other words, identification of the cause of a particular cancer promoting event does not necessarily guarantee a definitive treatment by targeting against that cause, even that may be a sufficient condition. Therefore, identifying the necessary events, not the sufficient causes, is imperative to obtain a real persistent treatment. In terms of targeting cancer metabolism, the prerequisite metabolic routes satisfying the criteria are expected to be identified as necessary for the growth of cancer cells, and no alternative detours could be adopted by compensation. Building up a type of capability is important to achieve this, as it may help discriminating each individual metabolic event in the cell and understand the driving force of metabolic reprogramming. In this review, the global landscape of cellular metabolism was revisited, especially focusing on the basic principles encoded in the chemical nature of the metabolic reactions.

Metabolic transformations are actually chemical reactions characterized by the transfer of electrons between reactors. In mammalian cells, the number of metabolic reactions is large, and it could form a network. However, no matter how complicated the situation of the metabolism is, the total amount of electrons released from the whole set of the reactions is eventually transferred to oxygen as mediated by the electron transport chain (ETC) and must be conserved (Fig. 1A). Even the electrons could be translocated spatially and between acceptors (Fig. 1B). Here, an electron balance model for proliferating cells was built on the basis of the basic law of electron conservation. In this model, we first made an assignment system for all common biomolecules involved in metabolism, by which a numeric value is endowed for each molecule in accordance with its potential to serve as a donor or receiver of electrons. This type of value was then applied for all the reactors and products in metabolic reactions to calculate the net value changes in the reactions. The results showed that it could reasonably reflect the electrons required for a particular reaction. This model assisted in identifying the

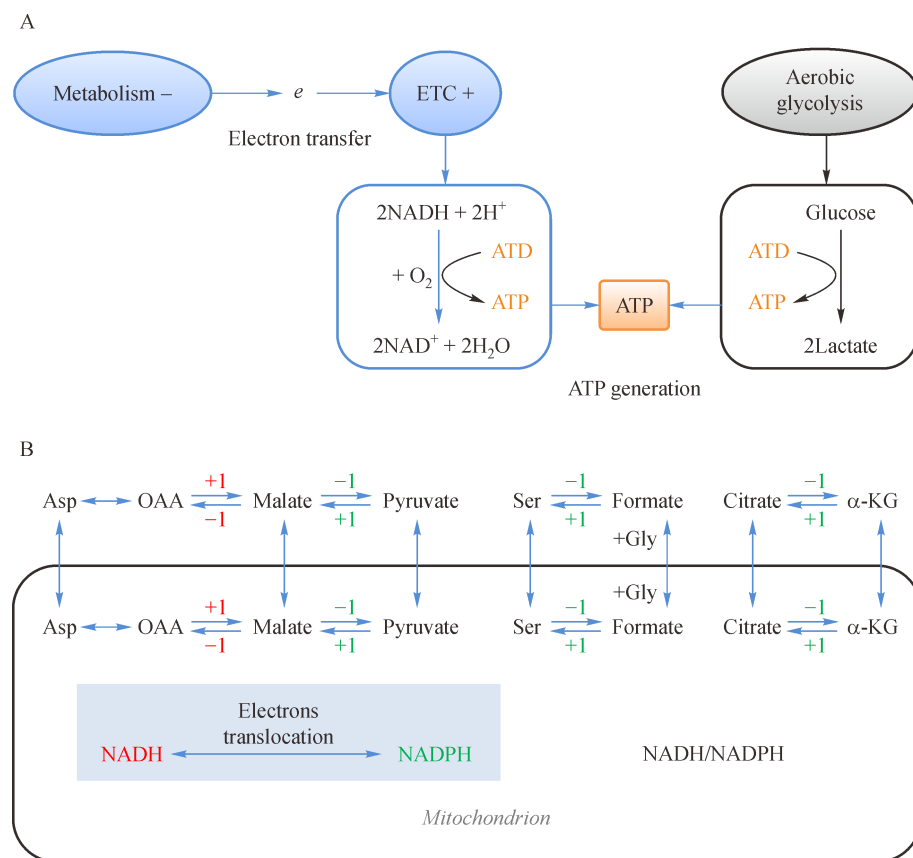


Fig. 1 Electron transfer and energy generation in cells. (A) Model for electron transfer and ATP generation. Cellular metabolism releases electrons for electron transport chain (ETC) to generate ATP, and aerobic glycolysis produces ATP without the involvement of electrons. (B) Translocation of electrons. Electrons in $\text{NADH} + \text{H}^+$ or $\text{NADPH} + \text{H}^+$ could be translocated spatially or to each other. “-,” production of electrons; “+,” dissipation of electrons; red number, $\text{NADH} + \text{H}^+$; green number, $\text{NADPH} + \text{H}^+$; black number, $\text{NADH} + \text{H}^+$ or $\text{NADPH} + \text{H}^+$.

pathways or conditions necessary or obligated for cell to choose for proliferation under hypoxia [27]. Some more interesting insights on cell metabolism were discussed in the present study, with special emphases on the introduction and utilization of electron transfer as the concept or tool key to describe some basic phenomena in cell biology, and further extended it to discuss some other important phenomena, including the Warburg effect (aerobic glycolysis) in cell proliferation.

Equation of state of electrons required for transformations

With the presence of multiple pathways for a particular metabolic event, one may ask if determinant factors for making the selective decisions exist. As a chemical reaction potentially involves electron transfer that depends on the number of valence electrons, a method to evaluate the relative capability of electron donation for biomolecules in general was designed in this study. The number of valence electrons of each single atom of the molecule was added together, disregarding the structure complexity nor the real donating consequence of the molecule in any type of reaction, and this value was nominated as the relative potential of electron transfer (PET), symbolized by "Y." Therefore, for a particular biomolecule,

$$Y = 4N_C + N_H - 3N_N - 2N_O, \quad (1)$$

where N_C , N_H , N_N , and N_O represent the atom number of carbon, hydrogen, oxygen, and nitrogen of metabolites, respectively, and 4, 1, -3 and -2 are the numbers of electrons each atom of the molecule could donate to reach

a full valence shell. In this manner, the Y values of CO_2 , H_2O , and NH_3/urea are equal to zero, and these were notably recognized as the end products of all bio-reactions. Therefore, Y could be recognized as a parameter reflecting the relative PET of a biomolecule in respect to the end point products.

When the Y value is applied to calculate the net change of this value in a reaction, a ΔY value which reflects the relative PET accompanied with a biochemical reaction, could be obtained.

$$\Delta Y_{P,S} = \sum_{j=1}^m Y_{P_j} - \sum_{i=1}^n Y_{S_i}, \quad (2)$$

where S and P are the carbon-containing substrates in the initial state and products in the final state, and $\sum_{j=1}^m Y_{P_j}$ and

$\sum_{i=1}^n Y_{S_i}$ represent the sums of Y of all the products and reactors of the reaction, respectively. As such, ΔY is the number of electrons required for the reaction. If PET change is negative, the transformation releases electrons. For the convenience of calculation, all metabolites could be reduced to the forms without derivatives, such as phosphate group, coenzyme, and tetrahydrofolic acid. Thus, Y could be recognized as a parameter of state, while ΔY is a function of state that could serve as a convenient calculation to evaluate the electron consumptions for a particular reaction (Table 1). In the metabolic system, ΔY only depends on the components of the initial substrates and final products regardless of the detailed metabolic routes [27]. Thus, it could exactly reflect the chemical nature of a metabolic transformation.

Table 1 The PET of metabolites

	Metabolites	Formula	Y	\bar{Y}
Carbohydrate	Glucose	$\text{C}_6\text{H}_{12}\text{O}_6$	24	4.00
	Ribose	$\text{C}_5\text{H}_{10}\text{O}_5$	20	4.00
	Fructose	$\text{C}_6\text{H}_{12}\text{O}_6$	24	4.00
	Glyceraldehyde	$\text{C}_3\text{H}_6\text{O}_3$	12	4.00
	Glyceric acid	$\text{C}_3\text{H}_6\text{O}_4$	10	3.33
	Pyruvate	$\text{C}_3\text{H}_4\text{O}_3$	10	3.33
	Lactate	$\text{C}_3\text{H}_6\text{O}_3$	12	4.00
	Oxaloacetate	$\text{C}_4\text{H}_4\text{O}_5$	10	2.50
	Malate	$\text{C}_4\text{H}_6\text{O}_5$	12	3.00
	Fumarate	$\text{C}_4\text{H}_4\text{O}_4$	12	3.00
	Succinate	$\text{C}_4\text{H}_6\text{O}_4$	14	3.50
	α -Ketoglutarate	$\text{C}_5\text{H}_6\text{O}_5$	16	3.20
	Citrate	$\text{C}_6\text{H}_8\text{O}_7$	18	3.00

(Continued)

	Metabolites	Formula	Y	\bar{Y}
Nucleobase	Adenine	C ₅ H ₅ N ₅	10	2.00
	Guanine	C ₅ H ₅ N ₅ O	8	1.60
	Cytosine	C ₄ H ₅ N ₃ O	10	2.50
	Thymine	C ₅ H ₆ N ₂ O ₂	16	3.20
	Uracil	C ₄ H ₄ N ₂ O ₂	10	2.50
Ribonucleoside	Adenosine	C ₁₀ H ₁₃ N ₅ O ₄	30	3.00
	Guanosine	C ₁₀ H ₁₃ N ₅ O ₅	28	2.80
	Cytidine	C ₉ H ₁₃ N ₃ O ₅	30	3.33
	Uridine	C ₉ H ₁₂ N ₂ O ₆	30	3.33
Deoxy-ribonucleoside	Deoxyadenosine	C ₁₀ H ₁₃ N ₅ O ₃	32	3.20
	Deoxyguanosine	C ₁₀ H ₁₃ N ₅ O ₄	30	3.00
	Deoxycytidine	C ₉ H ₁₃ N ₃ O ₄	32	3.56
	Deoxythymidine	C ₁₀ H ₁₄ N ₂ O ₅	38	3.80
Non-essential amino acids	Glycine	C ₂ H ₅ NO ₂	6	3.00
	Serine	C ₃ H ₇ NO ₃	10	3.33
	Aspartate	C ₄ H ₇ NO ₄	12	3.00
	Asparagine	C ₄ H ₈ N ₂ O ₃	12	3.00
	Glutamine	C ₅ H ₁₀ N ₂ O ₃	18	3.60
	Glutamate	C ₅ H ₉ NO ₄	18	3.60
	Alanine	C ₃ H ₇ NO ₂	12	4.00
	Proline	C ₅ H ₉ NO ₂	22	4.40
Semi-essential amino acids	Histidine	C ₆ H ₉ N ₃ O ₂	20	3.33
	Arginine	C ₆ H ₁₄ N ₄ O ₂	22	3.67
Essential amino acids	Threonine	C ₄ H ₉ NO ₃	16	4.00
	Cysteine ^a	C ₃ H ₇ NO ₂ S	16	5.33
	Methionine ^a	C ₅ H ₁₁ NO ₂ S	28	5.60
	Lysine	C ₆ H ₁₄ N ₂ O ₂	28	4.66
	Valine	C ₅ H ₁₁ NO ₂	24	4.8
	Leucine	C ₆ H ₁₃ NO ₂	30	5.00
	Isoleucine	C ₆ H ₁₃ NO ₂	30	5.00
	Tryptophan	C ₁₁ H ₁₂ N ₂ O ₂	46	4.18
	Phenylalanine	C ₉ H ₁₁ NO ₂	40	4.44
	Tyrosine	C ₉ H ₁₁ NO ₃	38	4.22
Acetyl-CoA	Acetate	C ₂ H ₄ O ₂	8	4.00
Lipid components	Glycerol	C ₃ H ₈ O ₃	14	4.67
	Palmitate	C ₁₆ H ₃₂ O ₂	92	5.75
	Farnesol ^b	C ₁₅ H ₂₆ O	84	5.60
End metabolites	Carbon dioxide	CO ₂	0	
	Water	H ₂ O	0	
	Urea/ammonia	CH ₄ N ₂ O/NH ₃	0	
Electron acceptor	Oxygen	O ₂	-4	

^aThe degree of reduction of sulphur is counted as +4.^bFarnesol (farnesyl pyrophosphate) is the precursor of sterols.

For the description of a chemical reaction, state equation is a powerful tool and has been wildly employed in the study of physical chemistry. For example, ΔG , ΔH , and ΔS are classical functions of state to calculate the net change of the free energy, enthalpy, and entropy of the reaction, respectively. However, in contrast to such thermodynamic

calculations, which are not readily measurable and further limited by the prerequisite conditions typically not satisfied in a complicated biological background, the calculation of ΔY is readily practical to be performed. Furthermore, by a straightforward calculation of ΔY , setting forth a direct estimation of the superiority for a particular reaction to take

place becomes possible, and this is in an order of hierarchy determined by the numeric values of ΔY . The reliability of such evaluation was tested in metabolic conditions and exemplified below.

Application of electron balance model for proliferating cells

The establishment of the function of ΔY for the description and evaluation of metabolic reactions was extended to a cellular background. To support proliferation, cells need to generate ATP and accumulate biomass. Besides inorganic ions (3%) that are unrelated to electron transfer, the macromolecules, including nucleic acids, sugars, proteins and lipids, their precursors and the related intermediates account for more than 96% of cell mass [28]. However, the

biosynthesis of macromolecules from their precursors does not involve electron transfer. Therefore, to build up the electron balance model, it only needs to take into account of ATP, and the precursors of nucleic acids (nucleotides), sugars (monosaccharides), proteins (non-essential amino acids) and lipids (fatty acids and glycerol) as the final cell state products, and the major carbon sources of glucose and glutamine as the initiate cell state substrates (Table 2). Given that electrons must keep conserved in an integrated cell, no matter how many reactions are involved and what types are, the sum of all ΔY should come to zero. Therefore,

$$\Delta Y_{\text{Cell}} = \sum \Delta Y_{\text{Metab}} + \sum \Delta Y_{\text{ETC}} = 0, \quad (3)$$

where $\sum \Delta Y_{\text{Metab}}$ and $\sum \Delta Y_{\text{ETC}}$ represent the sums of ΔY of all the reactions belonging to the metabolic and ETC categories, respectively. Based on the values in Table 2,

$$\begin{aligned} \sum \Delta Y_{\text{Metab}} = & \left\{ \left(\sum \Delta Y_{\text{Pyr-4,Glc}} + \sum \Delta Y_{\text{CO}_2-20,\text{Pyr}} / \sum \Delta Y_{\text{Lac+4,Pyr}} \right) ^{\text{ATP}} \right. \\ & + \left\{ \sum \Delta Y_{\text{Ribose-4,Glc}}^{\text{oPPP}} / \sum \Delta Y_{\text{Ribose-0,Glc}}^{\text{nPPP}} + \sum \Delta Y_{\text{Nuc-}} \right\} ^{\text{Nucleotide}} \\ & + \left\{ \sum \Delta Y_{\text{Sug-6,Gln}} / \sum \Delta Y_{\text{Sug-0,Glc}} \right\} ^{\text{Sugar}} \\ & + \left\{ \sum \Delta Y_{\text{Ser-8,Gln}} / \sum \Delta Y_{\text{Ser-2,Glc}} + \sum \Delta Y_{\text{Ala-6,Gln}} / \sum \Delta Y_{\text{Ala-0,Glc}} \right. \\ & + \sum \Delta Y_{\text{Asp-6,Gln}} / \sum \Delta Y_{\text{Asp-0,Glc}} / \sum \Delta Y_{(\text{Palm,Asp})+5.5,\text{Gln}} + \sum \Delta Y_{\text{Pro-2,Glc}} / \sum \Delta Y_{\text{Pro+4,Gln}} \left. \right\} ^{\text{Amino acid}} \\ & + \left\{ \sum \Delta Y_{\text{Glo-4,Gln}} / \sum \Delta Y_{\text{Glo+2,Glc}} \right. \\ & + \sum \Delta Y_{(\text{Palm,Asp})+5.5,\text{Gln}} / \sum \Delta Y_{(\text{Palm,Lac})+5.5,\text{Gln}} / \sum \Delta Y_{(\text{Palm,CO}_2)-6.5,\text{Gln}} \\ & \left. / \sum \Delta Y_{(\text{Palm,Asp})-0.5,\text{Glc}} / \sum \Delta Y_{(\text{Palm,Lac})-0.5,\text{Glc}} / \sum \Delta Y_{(\text{Palm,CO}_2)-12.5,\text{Glc}} \right\} ^{\text{Lipid}} \end{aligned}$$

The slash symbol means that electrons released from metabolic pathways depend on the substrates and products. In normal aerobic conditions, electrons are produced for the mitochondria to effectively generate ATP. Therefore, mitochondrial respiration essentially functions as a primary electron acceptor to enable metabolic transformations to process forward [29–31]. However, under the condition of hypoxia, such cost-effective mitochondrial ETC becomes disabled, which forces the metabolisms to be substantively rewired to take alternative pathways coupled with higher ΔY , as listed in Table 2.

Some rewired metabolic pathways could be easily identified using isotope-labeled glucose or glutamine, including the fermentation of pyruvate to lactate ($\sum \Delta Y_{\text{Lac+4,Pyr}}$), activated non-oxidative phosphate pentose pathway ($\sum \Delta Y_{\text{Ribose-0,Glc}}^{\text{nPPP}}$) (Fig. 2), increased glucose-derived glycerol 3-phosphate ($\sum \Delta Y_{\text{Glo+2,Glc}}$) and glutamine-derived proline ($\sum \Delta Y_{\text{Pro+4,Gln}}$), and glutamine-initiated lipogenesis ($\sum \Delta Y_{(\text{Palm,Asp})+5.5,\text{Gln}}$). By contrast, sugars, serine, and alanine are directly derived from glucose ($\sum \Delta Y_{\text{Sug-0,Glc}}$, $\sum \Delta Y_{\text{Ser-2,Glc}}$ and $\sum \Delta Y_{\text{Ala-0,Glc}}$). If glutamine is oxidized to provide electrons for mitochondrial ATP generation, glucose could be saved as carbon source to synthesize sugars, serine, or alanine, which is

essentially equivalent to that the carbon source was from glutamine. Therefore, glutamine could be diverted to reductive metabolism to avoid producing more electrons under hypoxia. All these hypoxia-associated metabolic preferences were experimentally tested in the previous paper [27] or supported by the works from other groups [4,14–18,32–34].

Finally, the coupled pathways were integrated and an equation for proliferating cells under hypoxia was obtained as follows:

$$\begin{aligned} \Delta Y_{\text{Cell}}^{\text{Hypo}} = & (\sum \Delta Y'_{\text{CAC-}} + \sum \Delta Y_{\text{Nuc-}} + \sum \Delta Y_{\text{Ser-2,Glc}}) \\ & + (\sum \Delta Y_{\text{Pro+4,Gln}} + \sum \Delta Y_{\text{Lip+,Gln}}) \\ = & 0 \end{aligned} \quad (4)$$

A notable detail that serine biosynthesis, from either glutamine or glucose, produces electrons, which are disadvantageous to cell growth under hypoxia based on this model. By contrast, many cancers rely on the uptake of nutritional serine for their proliferation [5,35,36]. Therefore, enforcing the unfavored *de-novo* synthesis of serine

Table 2 PET changes in metabolic transformations

Pathways	Initial substrates	Final products	ΔY
ATP generation	Electrons+4H ⁺ +O ₂	H ₂ O	$\Delta Y_{ETC} < 0$
	Glucose	Pyruvate	$\Delta Y_{Pyr-4,Glc} = -4$
	Pyruvate	CO ₂	$\Delta Y_{CO_2-20,Pyr} = -20$
	Pyruvate	Lactate	$\Delta Y_{Lac+4,Pyr} = +4$
	Citric acid cycle intermediates	CO ₂	$\Delta Y_{CAC-} < 0$
Nucleotide biosynthesis	Glucose	Ribose+CO ₂	$\Delta Y_{Ribose-4,Glc}^{oPPP} = -4$
	Glucose	Ribose	$\Delta Y_{Ribose_0,Glc}^{nPPP} = 0$
	Ribose+amino acids	Nucleotides	$\Delta Y_{Nuc-} < 0$
Sugar biosynthesis	Glutamine	Sugar	$\Delta Y_{Sug-6,Gln} = -6$
	Glucose	Sugar	$\Delta Y_{Sug_0,Glc} = 0$
Amino acid biosynthesis	Glutamine	Serine	$\Delta Y_{Ser-8,Gln} = -8$
	Glucose	Serine	$\Delta Y_{Ser-2,Glc} = -2$
	Glutamine	Alanine	$\Delta Y_{Ala-6,Gln} = -6$
	Glucose	Alanine	$\Delta Y_{Ala_0,Glc} = 0$
	Glutamine	Aspartate	$\Delta Y_{Asp-6,Gln} = -6$
	Glucose	Aspartate	$\Delta Y_{Asp_0,Glc} = 0$
	Glutamine	Proline	$\Delta Y_{Pro+4,Gln} = +4$
	Glucose	Proline	$\Delta Y_{Pro-2,Glc} = -2$
	Glutamine	Glycerol-3P	$\Delta Y_{Glo-4,Gln} = -4$
	Glucose	Glycerol-3P	$\Delta Y_{Glo+2,Glc} = +2$
Lipid biosynthesis	Glutamine	Palmitate+Aspartate	$\Delta Y_{(Palm,Asp)+5.5,Gln} = +5.5$
	Glutamine	Palmitate+Lactate	$\Delta Y_{(Palm,Lac)+5.5,Gln} = +5.5$
	Glutamine	Palmitate+CO ₂	$\Delta Y_{(Palm,CO_2)-6.5,Gln} = -6.5$
	Glucose	Palmitate+Aspartate	$\Delta Y_{(Palm,Asp)-0.5,Glc} = -0.5$
	Glucose	Palmitate+Lactate	$\Delta Y_{(Palm,Lac)-0.5,Glc} = -0.5$
	Glucose	Palmitate+CO ₂	$\Delta Y_{(Palm,CO_2)-12.5,Glc} = -12.5$

could hinder cell proliferation under hypoxia, the putative *in-vivo* tumor micro-environment. Such speculation is well supported by recent reports that showed that dietary restriction of serine and glycine indeed suppresses tumor growth in mouse models [36,37] by increasing the generation of ROS, an indicator of overproduced electrons [38]. In addition, serine is catabolized to provide 10-formyltetrahydrofolate for the biosynthesis of nucleotides and releases electrons and thus could potentially deteriorate electron transfer when the ETC is out of operation [39]. However, based on Equation (4), the processes of glutamine-initiated lipogenesis and proline biosynthesis could essentially function as the major substitutive electron acceptors under hypoxia [27].

Metabolic equivalent of glutamine-associated metabolic reactions

Cells could adapt to hypoxia by initiating glutamine-derived lipid and/or proline biosynthesis [27]. In the present study, the overall ΔY value for the metabolic

equivalent of glutamine-associated metabolic reactions (GMR) is denoted as

$$\Delta Y_{GMR} = \Delta Y_{Pro+4,Gln} + \Delta Y_{Palm+5.5,Gln}$$

where palmitate is used for quantitation. The available glutamine could be synthesized to either palmitate or proline to dissipate electrons under hypoxia. Considering the energy consumption,

$$\Delta Y_{GMR} = \Delta Y_{Palm+5.5,Gln} = +5.5 \text{ (with } \Delta Y/\text{ATP} = +2.93\text{)}$$

$$\text{or } \Delta Y_{GMR} = \Delta Y_{Pro+4,Gln} = +4 \text{ (with } \Delta Y/\text{ATP} = +4\text{)}$$

Apparently, the conversion of glutamine to proline is more cost-effective, although it dissipates less electrons compared with glutamine-initiated fatty acid synthesis. Therefore, in some cases, cells could opt for a preferential conversion of the glutamine to proline. Scavenging nutritional lipids or synthesizing the lipids from other carbon sources is then necessary. Given that acetyl-CoA is the precursor of fatty acids, ΔY_{GMR} now depends on the synthesis of acetyl-CoA from other nutrients. Thus,

$$\begin{aligned}\Delta Y_{\text{GMR}} &= \Delta Y_{\text{Pro}+4,\text{Gln}} + \Delta Y_{\text{Palm}+3.5,\text{Ac}} + \Delta Y_{\text{Ac,Nutr}} \\ &= +7.5 + \Delta Y_{\text{Ac,Nutr}}\end{aligned}\quad (5)$$

As listed in Table 3, some nutrients have a positive ΔY_{GMR} . In particular, acetate with $\Delta Y_{\text{GMR}} = +7.5$ is higher than glutamine with $\Delta Y_{\text{GMR}} = +4 + 5.5$ and thus could be preferentially utilized for lipogenesis under hypoxia [20,22]. In addition, leucine with $\Delta Y_{\text{GMR}} = +5.5$ (Table 3) could be an alternative carbon source for lipid biosynthesis and bias used by cancer cells [10,11]. Although these metabolic pathways could be cell type-specific and context-dependent, all of them are centered on the biosynthesis of lipid and proline.

When glutamine carbon is used for lipogenesis, its nitrogen could be used for the biosynthesis of amino acids or the secretory dihydroorotate if beyond the demand [18]. However, if glutamine is synthesized to the secretory proline, cells need to acquire sufficient nitrogen source for amino acid synthesis. Among the amino acids, alanine could be converted to excretory lactate after providing nitrogen with $\Delta Y = 0$. Therefore, as the second most abundant amino acid in human blood, alanine is the ideal nitrogen source and could be the favorite for *in-vivo* tumor cells [9].

Aerobic glycolysis results from energy demand and electron balance

Despite the extensive studies on aerobic glycolysis, also termed the Warburg effect, a serious lack of clarity regarding its ontology still exists [40]. In the present study, metabolic model based on energy requirement and electron balance was built to address the issue of lactate excretion of cells even under normal conditions (Fig. 3A). ATP energy is generated by glycolysis and mitochondrial respiration, termed as E_g and E_r , respectively. Balancing electrons transferred between intracellular transformations is required. Here, the conversion of glucose to the end product, lactate, or CO_2 is denoted as catabolism, while all other metabolic reactions are referred to as anabolism. Electrons produced by catabolism ($\sum \Delta Y_{\text{Cat}}$) and anabolism ($\sum \Delta Y_{\text{Ana}}$) should be equal to those dissipated by the ETC ($\sum \Delta Y_{\text{ETC}}$). Thus,

$$\sum \Delta Y_{\text{Cat}} + \sum \Delta Y_{\text{Ana}} + \sum \Delta Y_{\text{ETC+}} = 0 \quad (6)$$

Electrons produced by glucose catabolism rely on the detailed metabolic pathway. If glycolytic pyruvate is completely oxidized to CO_2 through the citric acid cycle (CAC), one mole of glucose could produce 24 moles of electrons. Alternatively, upon fermentation, glucose does not release electron. Therefore, the value of ΔY_{Cat} ranges from -24 to 0. There is a notable detail that $\sum \Delta Y_{\text{ETC+}}$ has

the extrema, ranging from 0 to the maximum, that is determined by the robustness of ETC, such as the normal expression and function of mitochondrial proteins and the availability of oxygen. When HeLa cells were treated with antimycin A, glucose oxidation through the CAC was totally blocked [27]. In such condition, $\Delta Y_{\text{ETC}} = 0$ and $\Delta Y_{\text{Cat}} = 0$, and thus, the reprogrammed $\Delta Y_{\text{Ana}} = 0$. On the basis of Equation (4), ΔY_{Ana} was substantially enhanced to ΔY_{Ana} [27]. Therefore, $\Delta Y_{\text{Ana}} < 0$, indicating that cellular anabolism releases electrons under normal condition.

As for non-proliferating cells, cellular anabolism is inactive and glucose catabolism mainly provides electrons ($\sum \Delta Y_{\text{Cat}}$) for mitochondrial energy generation (Fig. 3A). When cells are proliferating, anabolism-produced electrons ($\sum \Delta Y_{\text{Ana}}$) also fuel the ETC and compete with those from catabolism, which forces the fermentation of a part of glucose (Fig. 3B). Meanwhile, they need more ATP for biosynthesis [41], but the electron-consuming ability of the mitochondria in proliferating cells is even reduced due to the decreased mitochondrial protein levels [42] or limited by the mitochondrial ATP synthesis ability [43]. Therefore, the additional energy (ΔE) should be provided by additional glycolysis (aerobic glycolysis) due to the saturated mitochondrial activity. This speculation was supported by a recent report, which showed that increasing ATP demand by activating membrane pumps resulted in an increase in aerobic glycolysis, but it did not affect oxidative phosphorylation [44]. On the account of the saturated ETC, the mutual exclusion of electron dissipation could readily lead to a compromise: glucose catabolism partially shifting to fermentation to avoid electron production (aerobic glycolysis) and anabolism partially reprogrammed to reduce electron production according to the electron balance model. Therefore, concomitantly with aerobic glycolysis, metabolic reprogramming usually also occurs in proliferating cells. The extent metabolism reprogrammed to could be cell context-dependent, thus giving rise to metabolic heterogeneity. Whether aerobic glycolysis is the cause or outcome of cell proliferation has been long debated. In fact, a mutual causality apparently exists between them based on the model (Fig. 3). Proliferation-associated anabolism generates electrons for the mitochondria to push aerobic glycolysis. Meanwhile, aerobic glycolysis reserves mitochondrial space for cell proliferation. Summarily, for the reason of electron balance, aerobic glycolysis results from and contributes to cell proliferation.

A flux balance of glucose metabolism recently suggested that the demand of regenerating NAD^+ from NADH produced in glycolysis and serine biosynthesis leads to aerobic glycolysis [45]. In the present study, the electron balance model successfully revealed the chemical mechanism underlying aerobic glycolysis that essentially resulted from energy requirement and electron balance (Fig. 3).

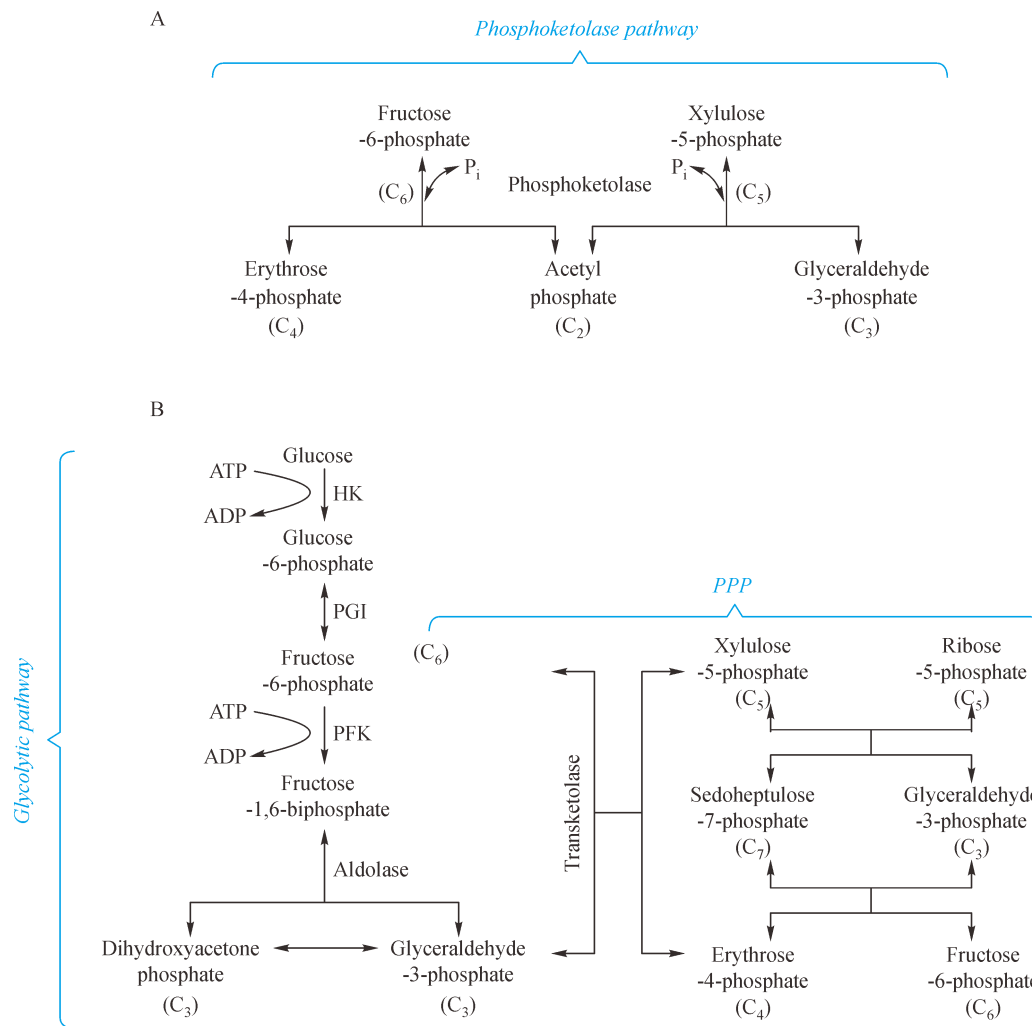


Fig. 2 Sugar metabolism. (A) Bacterial phosphoketolase pathway. Xylulose-5-phosphate/fructose-6-phosphate phosphoketolase (Xfp) catalyzes the production of acetyl phosphate (C_2) from the breakdown of xylulose-5-phosphate (C_5) or fructose-6-phosphate (C_6). Glyceraldehydes-3-phosphate (C_3) or erythrose-4-phosphate (C_4) is simultaneously generated. (B) Glycolysis and pentose phosphate pathway (PPP). In the glycolytic pathway, glucose is converted to fructose-1,6-biphosphate (C_6) that is further split by aldolase into dihydroxyacetone phosphate (C_3) and glyceraldehydes-3-phosphate (C_3). In PPP, glyceraldehydes-3-phosphate (C_3), erythrose-4-phosphate (C_4), xylulose-5-phosphate (C_5), ribose-5-phosphate (C_5), fructose-6-phosphate (C_6), and sedoheptulose-7-phosphate are produced by transketolase or transaldolase.

\bar{Y} and γ , same value but different significance in biology

The Y value of a molecule is divided by the number of carbon presented in that molecule to obtain \bar{Y} (Y per carbon) to establish a relative comparison of the PET evaluation between molecules of different sizes, reflecting here an average relative PET per carbon of the molecule when all carbons are supposed to be converted to the end-product CO_2 . Interestingly, a very similar type of value called *degree of reduction* (symbolized as γ) has been used by researchers in the field of bioprocess engineering, where the γ value is equal to the \bar{Y} value in the present study and defined as “the number of equivalents of available

electrons per gram atom C” [46]. Therefore, γ is essentially made to reflect the element balance in a bioprocess and used to calculate and predict the growth yields of bio-products in aerobic fermentations. However, when Y is applied to calculate the net change of this value in a reaction, a ΔY value, which reflects the electrons required for a biochemical reaction, could be obtained. By contrast, the value of \bar{Y} of the metabolites seems to bear key intrinsic characteristics and could be categorized by a cutoff value of “4.”

Token of “4” in the organic system

First, as for all the essential amino acids (Table 1), cysteine

Table 3 Metabolic equivalent of nutrients

Nutrients	Products	ΔY	$\Delta Y_{Ac,Nutr}$	ΔY_{GMR}
Acetate	Ac-CoA	0	0	+7.5
Leucine	3Ac-CoA	-6	-2	+5.5
Glucose	2Ac-CoA	-8	-4	+3.5
Lactate	Ac-CoA	-4	-4	+3.5
Alanine	Ac-CoA	-4	-4	+3.5
Aspartate	Ac-CoA	-4	-4	+3.5
Tyrosine	3Ac-CoA	-14	-4.67	+2.83
Phenylalanine	3Ac-CoA	-16	-5.33	+2.17
Tryptophan	3Ac-CoA+Formyl-THF	-18	-6	+1.5
Lysine	2Ac-CoA	-12	-6	+1.5
Isoleucine	2Ac-CoA	-14	-7	+0.5

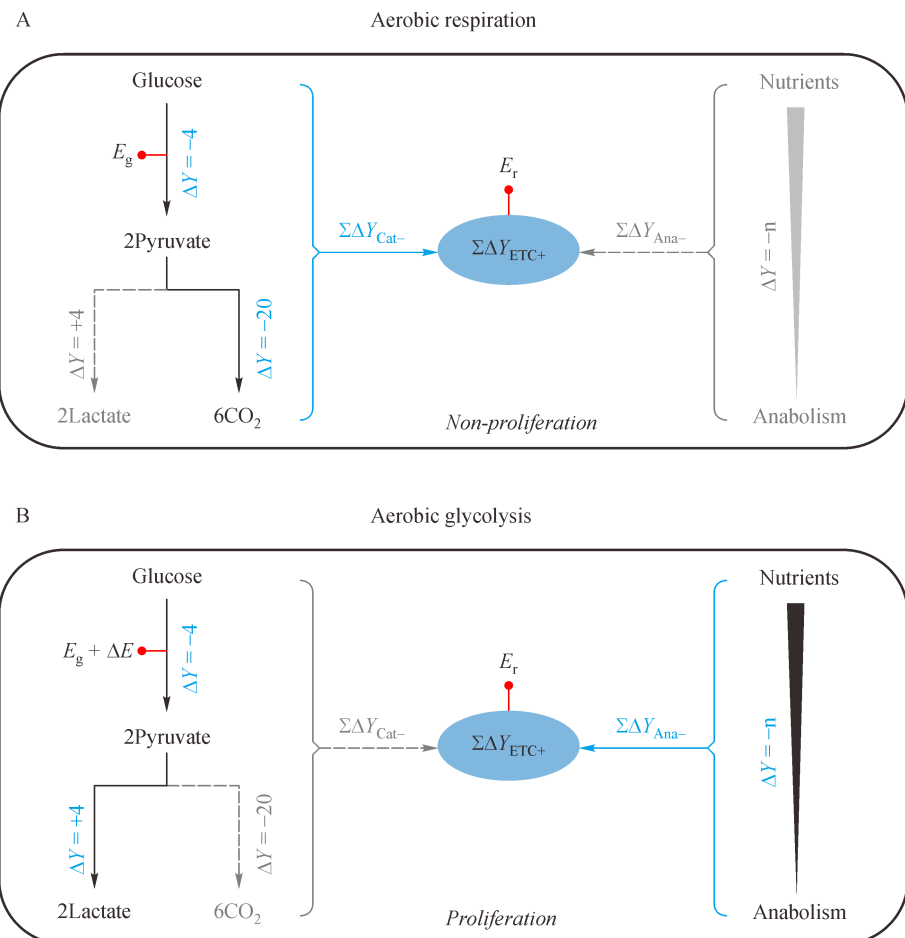
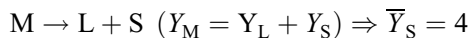


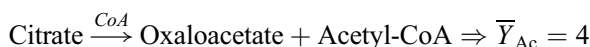
Fig. 3 Aerobic glycolysis results from energy requirement and electron balance. (A) In non-proliferating cells, anabolism is inactive and glucose is mainly oxidized to carbon dioxide through glycolysis and the citric acid cycle. Glucose catabolism produces electrons for mitochondrial ATP generation. (B) In proliferating cells, anabolism is active and produces electrons that could enter the mitochondria. By contrast, glucose is fermented to lactate to avoid electron production. E_r , ATP generation from mitochondrial ETC; E_g , ATP generation from glycolysis; ΔE , additional ATP required for anabolic transformations.

and tyrosine are counted as essential amino acids because of their biosynthesis from essential amino acids methionine and phenylalanine, and their \bar{Y} values are ≥ 4 . By contrast, the \bar{Y} values of non-essential amino acids are less than 4, with the exception of alanine and proline. Two semi-essential amino acids (histidine and arginine) that could be conditionally *de novo* synthesized have low \bar{Y} values (< 4) but high Y values (Table 1). Alanine and proline are the only amino acids that could be easily *de novo* synthesized, but they have a high \bar{Y} value (≥ 4) in human cells (Table 1). Similarly, lactate and lipid components, including glycerol, palmitate, and farnesol (sterol precursor, Table 1), have \bar{Y} values ≥ 4 , but they could be readily *de novo* synthesized. The chemical analyses and experimental results showed that cancer cells produce lactate to reduce the production of electrons, synthesize proline to excrete intracellular electrons with the help of alanine, and make lipids to increase the consumption of electrons [27]. Unfortunately, these non-essential metabolites with \bar{Y} values ≥ 4 , including lactate, proline, lipid, and alanine, are actively made or abnormally used by tumor cells [9,25,47]. These metabolic pathways with " $\bar{Y} \geq 4$ " are fully excavated by and indispensable for cancer cells to ensure electron transfer under hypoxia. Therefore, the metabolic pathways with " $\bar{Y} \geq 4$ " support cell proliferation under hypoxia and thus are indispensable to the progress of tumor cells *in vivo*. The specific metabolic characteristics may be used to guide the diagnosis and treatment of tumors.

Second, when the carbon chain of a metabolite (M) is split into two products without electron gain, one with shorter carbon chain (S, not CO_2) and the other with longer carbon chain (L), \bar{Y}_S seems to be 4.

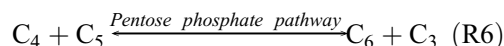
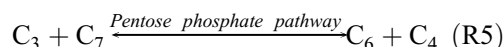
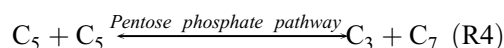
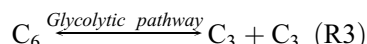
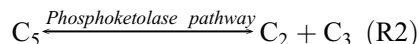
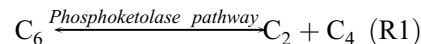


S could be one-carbon unit C_1 carried by tetrahydrofolic acid ($C_1\text{-THF}$) or two-carbon unit acetyl group by coenzyme A (acetyl-CoA). For example,



Serine is converted by serine hydroxymethyltransferase to glycine and methylenetetrahydrofolate ($C_1\text{-THF}$). Citrate is lysed by ATP citrate lyase (ACL) to oxaloacetate and acetyl-CoA. Upon β -oxidation, fatty acids are processed to β -ketoacyl-CoA that is ready to be cleaved by β -ketothiolase to release acetyl-CoA [48]. The \bar{Y} of sugars ($C_nH_{2n}O_n$) is 4, and their two- or three-carbon

groups could be reversibly split out or translocated between each other without the involvement of electron transfer. These processes take place in the bacterial phosphoketolase pathway [49] (R1 and R2, detailed in Fig. 2A), occur in the glycolytic pathway [48] (R3, detailed in Fig. 2B), or are featured in the pentose phosphate pathway [48] (R4–R6, detailed in Fig. 2B). The conversions produce saccharides with different carbon atoms.



The number 4 seems to be the tag \bar{Y} value for a split unit from metabolite transformations without electron gain. This phenomenon may be related to the chemical characteristics of carbon. The carbon atom with four valence electrons could have a stable electron configuration by losing or obtaining four electrons in chemical reactions. It serves as an optimized organizing center for an organic molecule to build up, because based on the stable outer shell electron configuration as eight, four valence electrons provide the highest possibility for a single atom to combine with as more other atoms as possible. This phenomenon is critical not only for the satisfaction in generating versatile structures for organic molecules but also for the stability of the molecules once formed. This may also provide the foundation as to why carbon is selected as the backbone for life in evolution. Taken together, the analysis of Y and \bar{Y} may help look at life science more closely from the perspective of its chemical nature. It may also be useful in piloting valuable approaches for cancer diagnosis and treatment.

Metabolic reprogramming, cancer metastasis, and cancer treatments

Based on all of the above, lipogenesis could be rewired to function as the major electron-dissipated pathway. Therefore, to enable electron transfer in hypoxic microenvironments, *in-vivo* tumor cells could potentially elevate lipid biosynthesis from glutamine or other carbon sources, such as acetate and leucine, and even store them as lipid droplets if beyond the requirements for biomass accumulation, particularly in malignant tumors [7,50–53]. Lipid droplets

consist of variable lipid and protein components, and they are swaddled with a single layer of phospholipids, thus considered as the organelles [50]. Cells may also take up some kinds of lipids to form a stable fat storage compartment [54,55]. In addition, tumor cells could scavenge the surrounding proteins as the source of amino acids [56] due to the poor vasculature usually associated with physiological hypoxia. Such harsh conditions may render tumor cells to detach from the lesions and thus initiate metastasis. Once the detached single cells move into the vessels, they could not efficiently absorb glucose for energy generation due to the impaired glucose transporters [57] that immersed in the blood with abundant glucose and oxygen. In this stage, these cruising cells turn to energy generation from oxidative phosphorylation of fatty acids [57–59]. As such, metabolic reprogramming could promote cancer metastasis by untiring cells and providing energy storage for their moving.

On the basis of the established model, electron transfer-driven metabolic reprogramming was mainly achieved by enhancing aerobic glycolysis, proline biosynthesis, and glutamine-initiated lipid syntheses. The involved critical enzymes could be the potential targets, including glycolytic enzymes [60,61]; P5CS and P5CR1/2 in proline biosynthesis pathway [12,27]; ACSS1/2, ACL, and BCAT1/2 in the biosynthesis of acetyl-CoA from acetate, citrate and leucine [11,19,21,62]; and ACC1/2 and HMGR, the rate-limiting enzymes in the biosynthesis of lipids, mainly fatty acids and sterols [63,64]. Metabolic reprogramming could be regulated and maintained by numerous signal transduction pathways, including Ras, Myc, and HIF1-mediated typical cascades, with a high degree of heterogeneity in cancer cells [24,25,65]. In particular, the hypoxia-associated HIF1 α signal could facilitate glucose fermentation [66], brake the citrate acid cycle by inactivating α -KGDH and PDH [67,68], and decrease oxidative PPP while increasing non-oxidative PPP [69]. These resultant actions restrict electron production. In addition, HIF1 induces FASN expression to promote lipogenesis to consume electrons [70]. Importantly, by bypassing these intricate and interchangeable cascades, electron transfer under hypoxia could be readily controlled through a cocktail of targets.

Conclusions

A metabolic flux concept of PET was put forward to profile the number of electrons that could be potentially released from cellular metabolites, and its state equation was defined. The state equation for metabolic transformations was derived on the basis of the law of conservation of electron in chemical reactions. Through the equivalent transformation, an electron balance model for proliferating cells was set up and further specified to describe hypoxic

cells. In particular, the model was expanded to uncover the origin and function of aerobic glycolysis. Proliferating cells have active anabolism that produces electrons. When the produced electrons are beyond the consumption ability of mitochondria under normal or hypoxic conditions, they provoke metabolic reprogramming to dissipate them according to the established model. Clearly, enabling electron transfer drives metabolic reprogramming. Therefore, this model conferred the chemical mechanism for and integrated major findings in metabolic reprogramming in cancers [24–26], and it is complementary to their molecular machineries. Importantly, this model helped identify the necessary conditions for cell proliferation under hypoxia and thus could guide the combinations of targets for cancers [27].

Acknowledgements

We would like to thank the members of Binghui Li's Lab for their suggestions and discussions. This work is supported by Grants from the National Natural Science Foundation of China (No. 81972567 to Binghui Li and No. 81772843 to Guoguang Ying), and Start Grant from Advanced Innovation Center for Human Brain Protection (to Binghui Li).

Compliance with ethics guidelines

Ronghui Yang, Guoguang Ying, and Binghui Li declare that they have no conflict of interest. This manuscript is a review article and does not involve a research protocol requiring approval by the relevant institutional review board or ethics committee.

References

1. Flier JS, Mueckler MM, Usher P, Lodish HF. Elevated levels of glucose transport and transporter messenger RNA are induced by ras or src oncogenes. *Science* 1987; 235(4795): 1492–1495
2. Wise DR, DeBerardinis RJ, Mancuso A, Sayed N, Zhang XY, Pfeiffer HK, Nissim I, Daikhin E, Yudkoff M, McMahon SB, Thompson CB. Myc regulates a transcriptional program that stimulates mitochondrial glutaminolysis and leads to glutamine addiction. *Proc Natl Acad Sci USA* 2008; 105(48): 18782–18787
3. Wise DR, Thompson CB. Glutamine addiction: a new therapeutic target in cancer. *Trends Biochem Sci* 2010; 35(8): 427–433
4. Sun C, Li T, Song X, Huang L, Zang Q, Xu J, Bi N, Jiao G, Hao Y, Chen Y, Zhang R, Luo Z, Li X, Wang L, Wang Z, Song Y, He J, Abliz Z. Spatially resolved metabolomics to discover tumor-associated metabolic alterations. *Proc Natl Acad Sci USA* 2019; 116(1): 52–57
5. Jain M, Nilsson R, Sharma S, Madhusudhan N, Kitami T, Souza AL, Kafri R, Kirschner MW, Clish CB, Mootha VK. Metabolite profiling identifies a key role for glycine in rapid cancer cell proliferation. *Science* 2012; 336(6084): 1040–1044
6. Zhu J, Thompson CB. Metabolic regulation of cell growth and

- proliferation. *Nat Rev Mol Cell Biol* 2019; 20(7): 436–450
7. Huang D, Li C, Zhang H. Hypoxia and cancer cell metabolism. *Acta Biochim Biophys Sin (Shanghai)* 2014; 46(3): 214–219
 8. Warburg O. On the origin of cancer cells. *Science* 1956; 123(3191): 309–314
 9. Sousa CM, Biancur DE, Wang X, Halbrook CJ, Sherman MH, Zhang L, Kremer D, Hwang RF, Witkiewicz AK, Ying H, Asara JM, Evans RM, Cantley LC, Lyssiotis CA, Kimmelman AC. Pancreatic stellate cells support tumour metabolism through autophagic alanine secretion. *Nature* 2016; 536(7617): 479–483
 10. Mayers JR, Wu C, Clish CB, Kraft P, Torrence ME, Fiske BP, Yuan C, Bao Y, Townsend MK, Tworoger SS, Davidson SM, Papagiannakopoulos T, Yang A, Dayton TL, Ogino S, Stampfer MJ, Giovannucci EL, Qian ZR, Robinson DA, Ma J, Sesso HD, Gaziano JM, Cochrane BB, Liu S, Wactawski-Wende J, Manson JE, Pollak MN, Kimmelman AC, Souza A, Pierce K, Wang TJ, Gerszten RE, Fuchs CS, Vander Heiden MG, Wolpin BM. Elevation of circulating branched-chain amino acids is an early event in human pancreatic adenocarcinoma development. *Nat Med* 2014; 20(10): 1193–1198
 11. Tönjes M, Barbus S, Park YJ, Wang W, Schlotter M, Lindroth AM, Pleier SV, Bai AHC, Karra D, Piro RM, Felsberg J, Addington A, Lemke D, Weibrech I, Hovestadt V, Rolli CG, Campos B, Turcan S, Sturm D, Witt H, Chan TA, Herold-Mende C, Kemkemer R, König R, Schmidt K, Hull WE, Pfister SM, Jugold M, Hutson SM, Plass C, Okun JG, Reifenberger G, Lichter P, Radlwimmer B. BCAT1 promotes cell proliferation through amino acid catabolism in gliomas carrying wild-type IDH1. *Nat Med* 2013; 19(7): 901–908
 12. Loayza-Puch F, Rooijers K, Buil LC, Zijlstra J, Oude Vrielink JF, Lopes R, Ugalde AP, van Breugel P, Hofland I, Wesseling J, van Tellingen O, Bex A, Agami R. Tumour-specific proline vulnerability uncovered by differential ribosome codon reading. *Nature* 2016; 530(7591): 490–494
 13. Liu W, Le A, Hancock C, Lane AN, Dang CV, Fan TW, Phang JM. Reprogramming of proline and glutamine metabolism contributes to the proliferative and metabolic responses regulated by oncogenic transcription factor c-MYC. *Proc Natl Acad Sci USA* 2012; 109(23): 8983–8988
 14. Hollinshead KER, Munford H, Eales KL, Bardella C, Li C, Escrivano-Gonzalez C, Thakker A, Nonnenmacher Y, Kluckova K, Jeeves M, Murren R, Cuozzo F, Ye D, Laurenti G, Zhu W, Hiller K, Hodson DJ, Hua W, Tomlinson IP, Ludwig C, Mao Y, Tennant DA. Oncogenic IDH1 mutations promote enhanced proline synthesis through PYCR1 to support the maintenance of mitochondrial redox homeostasis. *Cell Rep* 2018; 22(12): 3107–3114
 15. Mullen AR, Wheaton WW, Jin ES, Chen PH, Sullivan LB, Cheng T, Yang Y, Linehan WM, Chandel NS, DeBerardinis RJ. Reductive carboxylation supports growth in tumour cells with defective mitochondria. *Nature* 2012; 481(7381): 385–388
 16. Metallo CM, Gameiro PA, Bell EL, Mattaini KR, Yang J, Hiller K, Jewell CM, Johnson ZR, Irvine DJ, Guarente L, Kelleher JK, Vander Heiden MG, Iliopoulos O, Stephanopoulos G. Reductive glutamine metabolism by IDH1 mediates lipogenesis under hypoxia. *Nature* 2012; 481(7381): 380–384
 17. Wise DR, Ward PS, Shay JE, Cross JR, Gruber JJ, Sachdeva UM, Platt JM, DeMatteo RG, Simon MC, Thompson CB. Hypoxia promotes isocitrate dehydrogenase-dependent carboxylation of α -ketoglutarate to citrate to support cell growth and viability. *Proc Natl Acad Sci USA* 2011; 108(49): 19611–19616
 18. Wang Y, Bai C, Ruan Y, Liu M, Chu Q, Qiu L, Yang C, Li B. Coordinative metabolism of glutamine carbon and nitrogen in proliferating cancer cells under hypoxia. *Nat Commun* 2019; 10(1): 201
 19. Gao X, Lin SH, Ren F, Li JT, Chen JJ, Yao CB, Yang HB, Jiang SX, Yan GQ, Wang D, Wang Y, Liu Y, Cai Z, Xu YY, Chen J, Yu W, Yang PY, Lei QY. Acetate functions as an epigenetic metabolite to promote lipid synthesis under hypoxia. *Nat Commun* 2016; 7(1): 11960
 20. Schug ZT, Vande Voorde J, Gottlieb E. The metabolic fate of acetate in cancer. *Nat Rev Cancer* 2016; 16(11): 708–717
 21. Schug ZT, Peck B, Jones DT, Zhang Q, Grosskurth S, Alam IS, Goodwin LM, Smethurst E, Mason S, Blyth K, McGarry L, James D, Shanks E, Kalna G, Saunders RE, Jiang M, Howell M, Lassailly F, Thin MZ, Spencer-Dene B, Stamp G, van den Broek NJ, Mackay G, Bulusu V, Kamphorst JJ, Tardito S, Strachan D, Harris AL, Aboagye EO, Critchlow SE, Wakelam MJ, Schulze A, Gottlieb E. Acetyl-CoA synthetase 2 promotes acetate utilization and maintains cancer cell growth under metabolic stress. *Cancer Cell* 2015; 27(1): 57–71
 22. Kamphorst JJ, Chung MK, Fan J, Rabinowitz JD. Quantitative analysis of acetyl-CoA production in hypoxic cancer cells reveals substantial contribution from acetate. *Cancer Metab* 2014; 2(1): 23
 23. Comerford SA, Huang Z, Du X, Wang Y, Cai L, Witkiewicz AK, Walters H, Tantawy MN, Fu A, Manning HC, Horton JD, Hammer RE, McKnight SL, Tu BP. Acetate dependence of tumors. *Cell* 2014; 159(7): 1591–1602
 24. Boroughs LK, DeBerardinis RJ. Metabolic pathways promoting cancer cell survival and growth. *Nat Cell Biol* 2015; 17(4): 351–359
 25. Pavlova NN, Thompson CB. The emerging hallmarks of cancer metabolism. *Cell Metab* 2016; 23(1): 27–47
 26. Vazquez A, Kamphorst JJ, Markert EK, Schug ZT, Tardito S, Gottlieb E. Cancer metabolism at a glance. *J Cell Sci* 2016; 129(18): 3367–3373
 27. Liu M, Wang Y, Yang C, Ruan Y, Bai C, Chu Q, Cui Y, Chen C, Ying G, Li B. Inhibiting both proline biosynthesis and lipogenesis synergistically suppresses tumor growth. *J Exp Med* 2020; 217(3): e20191226
 28. Alberts B, Johnson A, Lewis J, Raff M, Roberts K, Walter P. Molecular Biology of the Cell. 5th edition. New York: Garland Science, 2008
 29. Titov DV, Cracan V, Goodman RP, Peng J, Grabarek Z, Mootha VK. Complementation of mitochondrial electron transport chain by manipulation of the NAD⁺/NADH ratio. *Science* 2016; 352(6282): 231–235
 30. Sullivan LB, Gui DY, Hosios AM, Bush LN, Freinkman E, Vander Heiden MG. Supporting aspartate biosynthesis is an essential function of respiration in proliferating cells. *Cell* 2015; 162(3): 552–563
 31. Birsoy K, Wang T, Chen WW, Freinkman E, Abu-Remaileh M, Sabatini DM. An essential role of the mitochondrial electron transport chain in cell proliferation is to enable aspartate synthesis. *Cell* 2015; 162(3): 540–551
 32. Mullen AR, Hu Z, Shi X, Jiang L, Boroughs LK, Kovacs Z, Boriack R, Rakheja D, Sullivan LB, Linehan WM, Chandel NS, DeBerardinis RJ. Oxidation of α -ketoglutarate is required for reductive

- carboxylation in cancer cells with mitochondrial defects. *Cell Rep* 2014; 7(5): 1679–1690
- 33. Li M, Lu Y, Li Y, Tong L, Gu XC, Meng J, Zhu Y, Wu L, Feng M, Tian N, Zhang P, Xu T, Lin SH, Tong X. Transketolase deficiency protects the liver from DNA damage by increasing levels of ribose 5-phosphate and nucleotides. *Cancer Res* 2019; 79(14): 3689–3701
 - 34. Li Q, Qin T, Bi Z, Hong H, Ding L, Chen J, Wu W, Lin X, Fu W, Zheng F, Yao Y, Luo ML, Saw PE, Wulf GM, Xu X, Song E, Yao H, Hu H. Rac1 activates non-oxidative pentose phosphate pathway to induce chemoresistance of breast cancer. *Nat Commun* 2020; 11(1): 1456
 - 35. Labuschagne CF, van den Broek NJ, Mackay GM, Vousden KH, Maddocks OD. Serine, but not glycine, supports one-carbon metabolism and proliferation of cancer cells. *Cell Rep* 2014; 7(4): 1248–1258
 - 36. Maddocks OD, Berkers CR, Mason SM, Zheng L, Blyth K, Gottlieb E, Vousden KH. Serine starvation induces stress and p53-dependent metabolic remodelling in cancer cells. *Nature* 2013; 493(7433): 542–546
 - 37. Gravel SP, Hulea L, Toban N, Birman E, Blouin MJ, Zakikhani M, Zhao Y, Topisirovic I, St-Pierre J, Pollak M. Serine deprivation enhances antineoplastic activity of biguanides. *Cancer Res* 2014; 74 (24): 7521–7533
 - 38. Maddocks ODK, Athineos D, Cheung EC, Lee P, Zhang T, van den Broek NJF, Mackay GM, Labuschagne CF, Gay D, Kruiswijk F, Blagih J, Vincent DF, Campbell KJ, Ceteci F, Sansom OJ, Blyth K, Vousden KH. Modulating the therapeutic response of tumours to dietary serine and glycine starvation. *Nature* 2017; 544(7650): 372–376
 - 39. Yang L, Garcia Canaveras JC, Chen Z, Wang L, Liang L, Jang C, Mayr JA, Zhang Z, Ghergurovich JM, Zhan L, Joshi S, Hu Z, McReynolds MR, Su X, White E, Morscher RJ, Rabinowitz JD. Serine catabolism feeds NADH when respiration is impaired. *Cell Metab* 2020; 31(4): 809–821.e6
 - 40. Liberti MV, Locasale JW. The Warburg effect: how does it benefit cancer cells? *Trends Biochem Sci* 2016; 41(3): 211–218
 - 41. Kilburn DG, Lilly MD, Webb FC. The energetics of mammalian cell growth. *J Cell Sci* 1969; 4(3): 645–654
 - 42. Slavov N, Budnik BA, Schwab D, Airoldi EM, van Oudenaarden A. Constant growth rate can be supported by decreasing energy flux and increasing aerobic glycolysis. *Cell Rep* 2014; 7(3): 705–714
 - 43. Luengo A, Li Z, Gui DY, Sullivan LB, Zagorulya M, Do BT, Ferreira R, Naamati A, Ali A, Lewis CA, Thomas CJ, Spranger S, Matheson NJ, Vander Heiden MG. Increased demand for NAD⁺ relative to ATP drives aerobic glycolysis. *Mol Cell* 2021; 81(4): 691–707.e6
 - 44. Epstein T, Xu L, Gillies RJ, Gatenby RA. Separation of metabolic supply and demand: aerobic glycolysis as a normal physiological response to fluctuating energetic demands in the membrane. *Cancer Metab* 2014; 2(1): 7
 - 45. Dai Z, Shestov AA, Lai L, Locasale JW. A flux balance of glucose metabolism clarifies the requirements of the Warburg effect. *Biophys J* 2016; 111(5): 1088–1100
 - 46. Shuler M, Kargi F, DeLisa M. Bioprocess Engineering: Basic Concepts. 3rd edition. Upper Saddle River, NJ: Prentice Hall, 2017
 - 47. Phang JM, Liu W, Hancock C, Christian KJ. The proline regulatory axis and cancer. *Front Oncol* 2012; 2: 60
 - 48. Berg JM, Tymoczko JL, Stryer L. Biochemistry. 7th edition. New York: W.H. Freeman, 2012
 - 49. Glenn K, Smith KS. Allosteric regulation of *Lactobacillus plantarum* xylose 5-phosphate/fructose 6-phosphate phosphoketolase (Xfp). *J Bacteriol* 2015; 197(7): 1157–1163
 - 50. Tirinato L, Pagliari F, Limongi T, Marini M, Falqui A, Seco J, Candeloro P, Liberale C, Di Fabrizio E. An overview of lipid droplets in cancer and cancer stem cells. *Stem Cells Int* 2017; 2017: 1656053
 - 51. Liu Q, Luo Q, Halim A, Song G. Targeting lipid metabolism of cancer cells: a promising therapeutic strategy for cancer. *Cancer Lett* 2017; 401: 39–45
 - 52. Medes G, Thomas A, Weinhouse S. Metabolism of neoplastic tissue. IV. A study of lipid synthesis in neoplastic tissue slices *in vitro*. *Cancer Res* 1953; 13(1): 27–29
 - 53. Ookhtens M, Kannan R, Lyon I, Baker N. Liver and adipose tissue contributions to newly formed fatty acids in an ascites tumor. *Am J Physiol* 1984; 247(1 Pt 2): R146–R153
 - 54. Balaban S, Nassar ZD, Zhang AY, Hosseini-Beheshti E, Centenera MM, Schreuder M, Lin HM, Aishah A, Varney B, Liu-Fu F, Lee LS, Nagarajan SR, Shearer RF, Hardie RA, Raftopoulos NL, Kakani MS, Saunders DN, Holst J, Horvath LG, Butler LM, Hoy AJ. Extracellular fatty acids are the major contributor to lipid synthesis in prostate cancer. *Mol Cancer Res* 2019; 17(4): 949–962
 - 55. Garcia-Bermudez J, Baudrier L, Bayraktar EC, Shen Y, La K, Guaracuco R, Yucel B, Fiore D, Tavora B, Freinkman E, Chan SH, Lewis C, Min W, Inghirami G, Sabatini DM, Birsoy K. Squalene accumulation in cholesterol auxotrophic lymphomas prevents oxidative cell death. *Nature* 2019; 567(7746): 118–122
 - 56. Palm W, Thompson CB. Nutrient acquisition strategies of mammalian cells. *Nature* 2017; 546(7657): 234–242
 - 57. Schafer ZT, Grassian AR, Song L, Jiang Z, Gerhart-Hines Z, Irie HY, Gao S, Puigserver P, Brugge JS. Antioxidant and oncogene rescue of metabolic defects caused by loss of matrix attachment. *Nature* 2009; 461(7260): 109–113
 - 58. Buchheit CL, Weigel KJ, Schafer ZT. Cancer cell survival during detachment from the ECM: multiple barriers to tumour progression. *Nat Rev Cancer* 2014; 14(9): 632–641
 - 59. Lee CK, Jeong SH, Jang C, Bae H, Kim YH, Park I, Kim SK, Koh GY. Tumor metastasis to lymph nodes requires YAP-dependent metabolic adaptation. *Science* 2019; 363(6427): 644–649
 - 60. Ganapathy-Kanniappan S, Geschwind JF. Tumor glycolysis as a target for cancer therapy: progress and prospects. *Mol Cancer* 2013; 12(1): 152
 - 61. Koppenol WH, Bounds PL, Dang CV. Otto Warburg's contributions to current concepts of cancer metabolism. *Nat Rev Cancer* 2011; 11 (5): 325–337
 - 62. Hatzivassiliou G, Zhao F, Bauer DE, Andreadis C, Shaw AN, Dhanak D, Hingorani SR, Tuveson DA, Thompson CB. ATP citrate lyase inhibition can suppress tumor cell growth. *Cancer Cell* 2005; 8 (4): 311–321
 - 63. Svensson RU, Parker SJ, Eichner LJ, Kolar MJ, Wallace M, Brun SN, Lombardo PS, Van Nostrand JL, Hutchins A, Vera L, Gerken L, Greenwood J, Bhat S, Harriman G, Westlin WF, Harwood HJ Jr, Saghatelian A, Kapeller R, Metallo CM, Shaw RJ. Inhibition of acetyl-CoA carboxylase suppresses fatty acid synthesis and tumor growth of non-small-cell lung cancer in preclinical models. *Nat Med*

- 2016; 22(10): 1108–1119
- 64. Stine JE, Guo H, Sheng X, Han X, Schointuch MN, Gilliam TP, Gehrig PA, Zhou C, Bae-Jump VL. The HMG-CoA reductase inhibitor, simvastatin, exhibits anti-metastatic and anti-tumorigenic effects in ovarian cancer. *Oncotarget* 2016; 7(1): 946–960
 - 65. Martinez-Outschoorn UE, Peiris-Pages M, Pestell RG, Sotgia F, Lisanti MP. Cancer metabolism: a therapeutic perspective. *Nat Rev Clin Oncol* 2017; 14(1): 11–31
 - 66. Doherty JR, Cleveland JL. Targeting lactate metabolism for cancer therapeutics. *J Clin Invest* 2013; 123(9): 3685–3692
 - 67. Sun RC, Denko NC. Hypoxic regulation of glutamine metabolism through HIF1 and SIAH2 supports lipid synthesis that is necessary for tumor growth. *Cell Metab* 2014; 19(2): 285–292
 - 68. Kim JW, Tchernyshyov I, Semenza GL, Dang CV. HIF-1-mediated expression of pyruvate dehydrogenase kinase: a metabolic switch required for cellular adaptation to hypoxia. *Cell Metab* 2006; 3(3): 177–185
 - 69. Shukla SK, Purohit V, Mehla K, Gunda V, Chaika NV, Vernucci E, King RJ, Abrego J, Goode GD, Dasgupta A, Illies AL, Gebregiworgis T, Dai B, Augustine JJ, Murthy D, Attri KS, Mashadova O, Grandgenett PM, Powers R, Ly QP, Lazenby AJ, Grem JL, Yu F, Matés JM, Asara JM, Kim JW, Hankins JH, Weekes C, Hollingsworth MA, Serkova NJ, Sasson AR, Fleming JB, Oliveto JM, Lyssiotis CA, Cantley LC, Berim L, Singh PK. MUC1 and HIF-1 α signaling crosstalk induces anabolic glucose metabolism to impart gemcitabine resistance to pancreatic cancer. *Cancer Cell* 2017; 32(1): 71–87.e7
 - 70. Furuta E, Pai SK, Zhan R, Bandyopadhyay S, Watabe M, Mo YY, Hirota S, Hosobe S, Tsukada T, Miura K, Kamada S, Saito K, Iizumi M, Liu W, Ericsson J, Watabe K. Fatty acid synthase gene is up-regulated by hypoxia via activation of Akt and sterol regulatory element binding protein-1. *Cancer Res* 2008; 68(4): 1003–1011